

Specular reflection of polar molecules from a simple multi-cylinder electrostatic mirror: a method for separating BaF molecules produced in a buffer-gas-cooled laser-ablation source from other ablation products

H.-M. Yau, Z. Corriveau, N. T. McCall, J. Perez Garcia, D. Heinrich, R. L. Lambo, G. K. Koyanagi, M. C. George, C. H. Storry, M. Horbatsch, and E. A. Hessels*

Department of Physics and Astronomy, York University

(EDM³ Collaboration)

(Dated: October 8, 2024)

A method for specular reflection of polar molecules is proposed. Electrostatic potentials and forces are calculated for a low-field-seeking molecule near a series of long cylindrical electrodes of radius r with dc potentials of $+V$ and $-V$ applied to alternate electrodes. A center-to-center separation of $2.9r$ leads to remarkably flat equipotential surfaces and thus to a nearly planar mirror for specular reflection of the polar molecules, with the angle of reflection equalling the angle of incidence to an accuracy approaching a microradian. This mirror can be used to redirect cryogenic molecular beams. Separating barium monofluoride (BaF) molecules created in a helium-buffer-gas laser-ablation source from other ablation products is a necessary step to producing a pure sample of matrix-isolated BaF, as is required by the EDM³ collaboration for implementing a precise measurement of the electron electric dipole moment. The design and modelling for the BaF deflector based on this electrode geometry is presented.

I. INTRODUCTION

The Stark shift of a neutral polar molecule leads to a potential energy and force for a molecule in an electrostatic field. These potentials depend on the magnitude of electric field, and can be low- or high-field seeking, depending on the molecule's rotational quantum number (and its projection) and on the magnitude of the electric field. Deflection of neutral polar molecules by electrostatic fields was first demonstrated [1] almost a century ago. For low-field-seeking states, a region of large electric field can be used to reflect polar molecules. [2–5]

In this work, we present a simple geometry that allows for an electrostatic polar-molecule mirror with specular reflections. Our geometry (see Fig. 1a) consists of a series of long cylindrical electrodes, rather than electrodes deposited on an insulating substrate used [2–4] in previous electrostatic mirrors. The cylindrical electrodes allow for reflections that are nearly specular. The lack of an insulating substrate avoids possible arcing between electrodes, allowing for larger voltages to be used. This arcing can be of particular concern for cryogenic molecules created in a laser-ablation buffer-gas source, given that over time laser-ablation products could coat the insulating substrate and create surface pathways for arcing.

With the cylinders having applied voltages of $+V$ and $-V$ (alternately, as in Fig. 1a) and, with a carefully chosen separation between the cylinders, the magnitude of the electric field decreases exponentially with distance from the mirror, but shows a remarkably small variation within the planes parallel to the mirror surface (Section II). This small variation is in contrast to previous

electrostatic mirrors [2–5], and is key to allowing for specular reflections.

Although the results of this work are generally applicable to any polar molecule, in Section III, we specialize to the case of barium monofluoride (BaF), since this molecule is being employed by the EDM³ collaboration in an attempt to make an ultraprecise measurement [6] of the electric dipole moment of the electron. For the measurement, BaF molecules produced by a buffer-gas-cooled laser-ablation source are embedded in solid argon [7] or neon [8–10]. For the precision measurement it is necessary to have an uncontaminated solid, and therefore the BaF molecules must be separated from all of the other ablation products via a deflection.

By careful choice of V , one can further improve the quality of the specular reflections. In the section IV, we describe how the electrostatic mirror will be used to deflect the BaF molecules away from the other ablation products.

II. ELECTRIC FIELD PROFILE

The Stark shift experienced by a slowly-moving polar molecule depends only on the magnitude of the electric field, since, even if the direction of the field is varying spatially, the orientation of the moving molecule follows the field direction adiabatically as it moves through the field. Therefore, an ideal electrostatic planar mirror would have constant field magnitudes on planes that are parallel to the mirror surface.

We consider here the simple geometry shown in Fig. 1(a), in which equally spaced long cylinders of radius r have a center-to-center separation s , and have potentials $+V$ and $-V$ applied to alternate cylinders. To calculate the electrostatic potential for this problem, one can

* hessels@yorku.ca

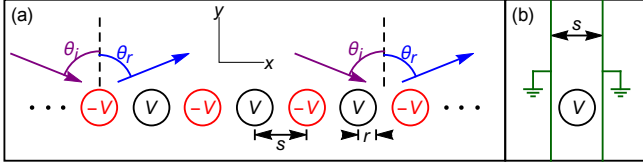


FIG. 1. (color online) The geometry being considered in this work uses a set of long cylindrical electrodes of radius r and center-to-center separation s that are alternately set to dc voltages of $+V$ and $-V$, as shown in cross section in panel (a). For the separation s pictured, reflections are almost perfectly specular (with angle of reflection, θ_r , equal to the angle of incidence, θ_i , independent of whether the incident molecule is aimed at the axis of one of the cylinders, (as pictured at the left in (a)), at a point halfway between two cylinders (as pictured at the right in (a)), or at any other point, x . By symmetry, the fields can be calculated from that of a single cylinder at potential $+V$ (or $-V$) centered between two grounded planes separated by s , as shown in panel (b).

use symmetry to reduce the problem to that of a single cylinder at potential V centered between two grounded planes, as shown in Fig. 1(b). This simplified geometry uses the fact that the planes bisecting two adjacent cylinders have an electrostatic potential of exactly zero.

The electrostatic potential for the Fig. 1(b) geometry can be calculated in two ways. First, one can numerically solve the two-dimensional Laplace equation with a boundary condition of V on the circle of radius r , centred in a grounded rectangle of width s and height $h \gg s$. With an extrapolation of h to infinity, this method allows for accurate calculations of the electrostatic potential.

An analytic solution is also possible, using line charges and the method of images. An initial line charge $+\lambda$ at $x = y = 0$ gives a uniform potential on the circle of radius r . Two image charges $-\lambda$ are needed (at $x = \pm s$, $y = 0$) to establish the grounded potentials at $x = \pm s/2$ (the green lines in Fig. 1(b)). With these two image charges, the potential on the central circle of radius r is no longer constant. However, this can be rectified with two additional line charges $+\lambda$ at $x = \pm r^2/s$, $y = 0$. These in turn need image charges to reinstate the grounded-plane boundary conditions. The result is an infinite number of image line charges (all in the $y = 0$ plane) whose locations can be expressed as continuing fractions:

$$x_{n_1 n_2 n_3 \dots n_N} = n_1 s + \frac{r^2}{n_2 s + \frac{r^2}{n_3 s + \frac{r^2}{n_4 s + \dots + \frac{r^2}{n_N s}}}}. \quad (1)$$

Here, N is an integer ≥ 1 , and the indices n_1 through n_N can take on all possible integer values except that n_2

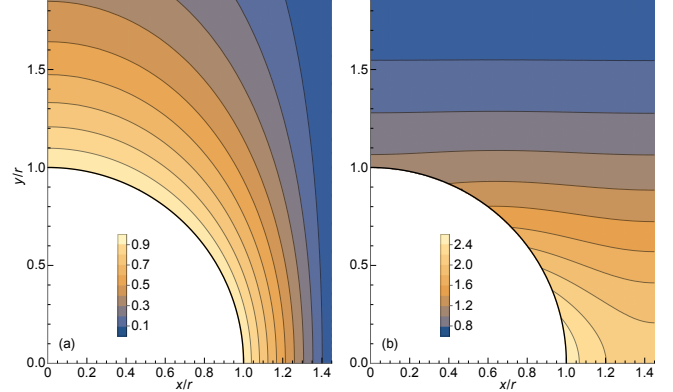


FIG. 2. (color online) The electrostatic potential is shown in (a) in units of V , and the electric field magnitude is shown in (b) in units of V/r . Both plots are for $s = 2.9r$, which leads to nearly horizontal contours of electric field magnitude for $y > r$, as seen in (b).

through n_N must be non-zero. The line charges all have charge densities of $\pm\lambda$, with

$$\lambda_{n_1 n_2 n_3 \dots n_N} = -\lambda(-1)^{N+\sum_{i=1}^N n_i}. \quad (2)$$

The electrostatic potential for the geometry in Fig. 1 is then given by

$$\Phi(x, y) = \frac{-\lambda}{2\pi\epsilon_0} \sum_{N=1}^{\infty} \sum_{n_1, n_2, \dots, n_N} (-1)^{N+\sum_{i=1}^N n_i} \times \ln(\sqrt{(x - x_{n_1 n_2 \dots n_N})^2 + y^2}), \quad (3)$$

where the value of λ is obtained from $\Phi(r, 0) = V$. The electric field magnitude is

$$|\vec{E}(x, y)| = \sqrt{\left(\frac{\partial \Phi}{\partial x}\right)^2 + \left(\frac{\partial \Phi}{\partial y}\right)^2} V = \frac{\sum_{N=1}^{\infty} \sum_{n_1, n_2, \dots, n_N} (-1)^{N+\sum_{i=1}^N n_i} \ln(\sqrt{x_{n_1 n_2 \dots n_N}^2 + r^2})}{\sum_{N=1}^{\infty} \sum_{n_1, n_2, \dots, n_N} \frac{(-1)^{N+\sum_{i=1}^N n_i} (x - x_{n_1 n_2 \dots n_N})}{\sqrt{(x - x_{n_1 n_2 \dots n_N})^2 + y^2}}^2 + \left(\sum_{N=1}^{\infty} \sum_{n_1, n_2, \dots, n_N} \frac{(-1)^{N+\sum_{i=1}^N n_i} y}{\sqrt{(x - x_{n_1 n_2 \dots n_N})^2 + y^2}}\right)^2}^{\frac{1}{2}}. \quad (4)$$

An approximation to this infinite sum can be had by a truncation that has equal number of positive and negative image line charges added inside the cylinder centred at $(x, y) = (0, 0)$.

The electrostatic potential and electric field magnitude for the case $s = 2.9r$ is shown in Fig. 2. For this choice of separation, the electric field magnitude contours (Fig. 2(b) for $y/r \gtrsim 1.4$) are nearly flat surfaces. For $s < 2.9r$, the field magnitude is larger at $x = s/2$ than it is at $s = 0$, and for $s > 2.9r$, the opposite is true.

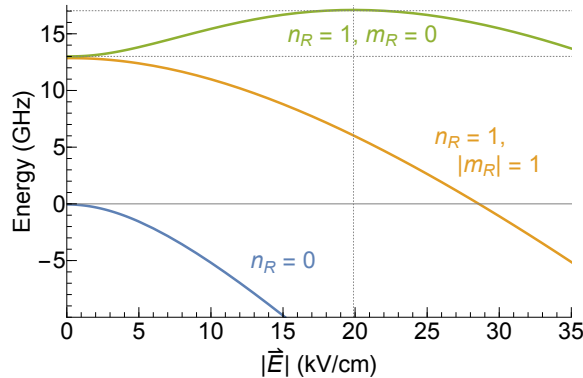


FIG. 3. (color online) The Stark shift of the lowest rotational levels of the ground electronic and vibrational state of the BaF molecule. Molecules in the $n_R=1$, $m_R=0$ state are low-field seeking for fields of up to 20 kV/cm, and it is molecules in this state that are used for our deflector.

III. STARK SHIFT AND MOLECULAR POTENTIAL ENERGY

To obtain the potential energy experienced by a polar molecule in the electric field of Section II, we need to use the Stark shift of the molecule. Any polar molecule could be used, however, we focus this work on the BaF molecule, since the BaF molecule is being used [6, 10] by the EDM³ collaboration.

The Stark shift of the lowest electronic and vibrational state of the BaF molecule has been discussed in Ref. [11], and is calculated using methods first presented in Ref. [12]. Fig. 3 shows the calculated energy levels of the lowest two rotational states in the presence of an electric field. For fields of 20 kV/cm or less, the $n_R=1$, $m_R=0$ state (here n_R is the rotational quantum number and m_R is its projection) is a low-field-seeking state.

Applying this Stark shift to the field of Fig. 2(b), with the field set to 20 kV/cm at a height of $y \approx 1.4r$ (where the contours of Fig. 2(b) become approximately flat), leads to the potential shown in Fig. 4. The strength of this potential is sufficient to reflect BaF molecules that have a downward velocity component of 4.5 m/s or less.

Note that the equipotential surfaces are very nearly planar, being even more planar than the surfaces of Fig. 2(b) since the 20 kV/cm field is tuned to the maximum shift, as shown in Fig. 3. Calculated trajectories show that reflections are nearly specular. In particular, for molecules produced in a helium-buffer-gas source (which would have a forward velocity of >100 m/s), all calculated trajectories have a difference between the angle of incidence and the angle of reflection of less than one microradian. Even for much slower molecules (≈ 5 m/s forward velocity), which would be hard to produce and would lead to reflections that are less grazing, this difference would still be $\lesssim 10$ microradians.

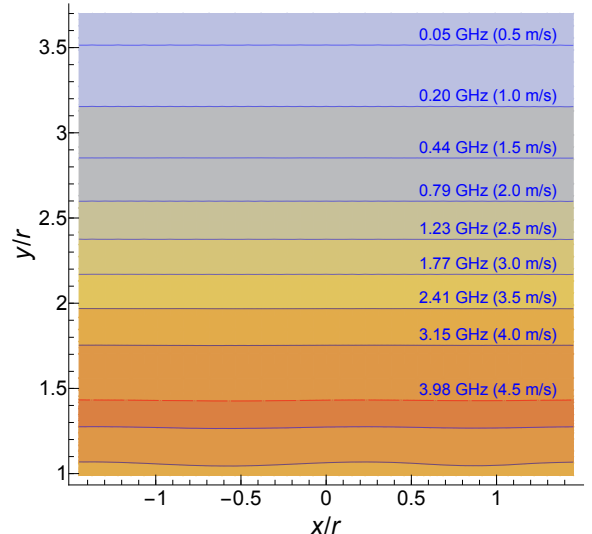


FIG. 4. (color online) The potential experienced by a BaF molecule in the $n_R=1$, $m_R=0$ state, which results from the Stark shift of Fig. 3 along with the electric field of Fig. 2(b). The potential on the electrodes is tuned to have a field of 20 kV/cm at a height of $y \approx 1.4r$. The downward velocity of a BaF molecule that can be reflected by each contour is indicated.

IV. OUR DESIGN FOR SEPARATING BaF MOLECULES FROM OTHER ABLATION PRODUCTS

Figure 5 shows our design that will be used to separate BaF molecules from other laser-ablation products. As our source uses ablated barium metal in the presence of SF₆ to produce BaF molecules in the buffer-gas cell, many other atoms (e.g., Ba), molecules (e.g., BaF₂, SF₆) and clusters (e.g., Ba_n) could be present. Ions are easily separated with a small electrostatic field. Our apparatus [10] leaves a 20-cm spacing between the laser-ablation buffer-gas source and the substrate on which the solid is grown. This 20-cm spacing is sufficient to allow small deflections possible from an electrostatic deflector, as described in this work, (or similar small deflections possible for laser-induced forces [13, 14]) to separate the BaF molecules from the other laser-ablation products. The large spacing between the buffer-gas source and the deflector and the efficient cryopumping by charcoal on the cryogenic surfaces allows for a low enough pressure near the deflector to make the effects of collisions minimal.

The design shown in Fig. 5 consists of a series of 27 1.5-mm-diameter stainless-steel cylinders that are alternately held at potentials of -2000 V (red) and +2000 V (blue) that create the required electric fields. Two razor-sharp stainless-steel blockers (b1 and b9 in Fig. 5) ensure that no atom, molecule, or cluster can travel directly from the 1-mm-high opening of the buffer-gas source to any point on the sapphire substrate. The sharp edges of the blockers ensure that BaF molecules do not make graz-

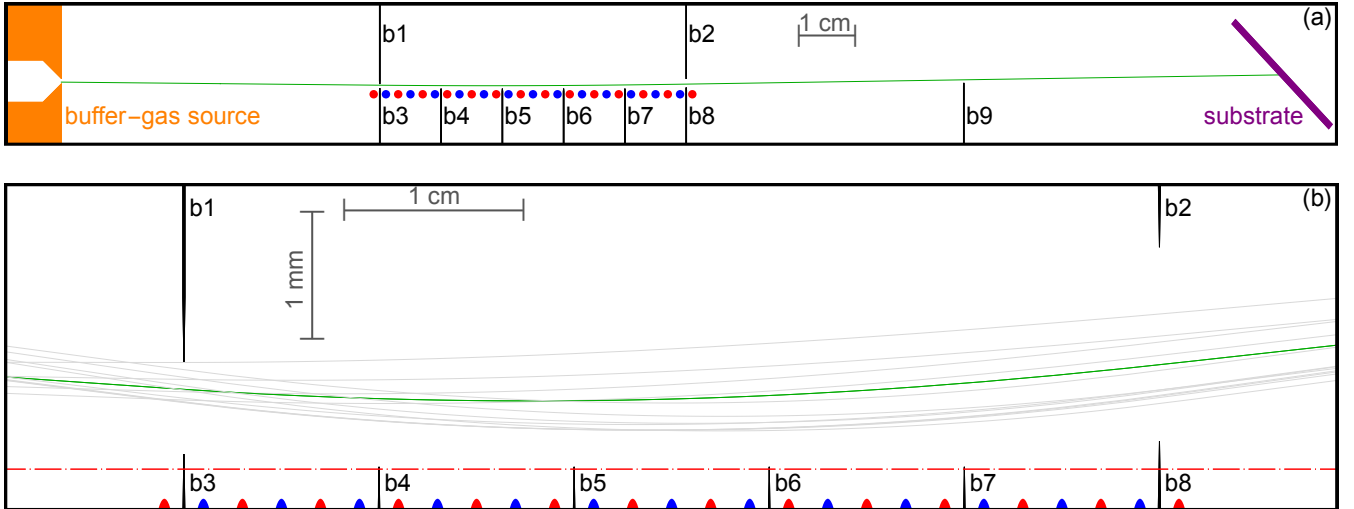


FIG. 5. (color online) The design for an electrostatic deflector for separating BaF molecules from other laser-ablation products (a). Panel (b) shows an expanded view of the central part of the apparatus, with the horizontal and vertical magnifications by factors of 3 and 30, respectively. Several trajectories (green and gray) are shown for BaF molecules in the $n_R = 1, m_R = 0$ state. The red dot-dash line represents the plane from which molecules with a downward velocity component of 4.5 m/s are reflected, as also shown in Fig. 4. Blockers b1 through b9 (which are razor sharp) ensure that there are no straight-line paths from the source to any part of the substrate. Additionally, they block both spectral and nonspectral reflection of molecules off the cylindrical electrodes (red and blue) from reaching the substrate.

ing reflections off of the blockers themselves. Additional blockers (b2 through b8) ensure that no reflections (spectral or nonspectral) off of the cylinders can make it to the substrate. The blockers are located in planes where the potential very nearly zero, resulting in very small disturbances of the potential due to their presence.

A typical trajectory for a deflected BaF molecule (in the $n_R=1, m_R=0$ state) is shown in panel (a) of the figure. Panel (b) shows an expanded view (expanded by a factor of 3 in the horizontal direction and a factor of 30 in the vertical direction) with a larger set of trajectories. Panel (b) also shows the surface of reflection for BaF molecules with a downward component of velocity of 4.5 m/s, represented by the dot-dashed line (as in Fig. 4).

A simulation of this deflection is performed for a thermal source of molecules with a 4-kelvin temperature and an average forward speed of 150 m/s (the typical speed for a helium buffer-gas source [15]). In the simulation, molecules start from the 1-mm-high output aperture of the buffer-gas source. Most molecules are intercepted by one of the blockers (b1 through b9 in Fig. 5), but molecules in the $n_R=1, m_R=0$ state that have initial downward velocity components of 0.1 to 3 m/s can be deflected onto the central one-millimeter-high band of the substrate. The simulation shows that the flux of $n_R=1, m_R=0$ molecules that are deflected to this band on the substrate is equal to 62% of the flux that would have been incident on the same area if there were no deflector present. Thus the deflector design is expected to efficiently deflect BaF molecules. No other atom, molecule or clusters created in the ablation source is expected to have a large enough permanent dipole moment or polar-

izability to be significantly deflected by the electric fields in this deflector.

To realize the 62% deflection efficiency, the BaF molecules would have to be optically pumped into the $n_R=1, m_R=0$ state. At 4 K, more than 70% of the molecules will be in the $n_R=0, 1, 2$ and 3 states. A laser driving transitions from the $X^2\Sigma_{1/2}(v=0, n_R=3)$ state to the $A^2\Pi_{1/2}(v=0, j=3/2)$ positive-parity state will move the $n_R=3$ population into the $n_R=1$ state. Two other lasers tuned to drive transitions from the $X^2\Sigma_{1/2}(v=0)$ states with $n_R=0$ and 2 to the $A^2\Pi_{3/2}(v=0, j=3/2)$ state will drive the $n_R=0$ and 2 populations into the $X^2\Sigma_{1/2}(v=0, n_R=1)$ state. The $A^2\Pi_{3/2}$ state is used since its very small lambda-doubling separation allows for mixing of odd- and even-parity states in even very small electric fields, allowing for decays to both odd- and even-parity states. A final laser beam (downstream of the others), this one in an applied electric field, is tuned to the transition from the $X^2\Sigma_{1/2}(v=0, n_R=1, |m_R|=1)$ state to the $A^2\Pi_{1/2}(v=0, j=1/2)$ positive-parity state to move the population into the $X^2\Sigma_{1/2}(v=0, n_R=1, m_R=0)$ state. The losses to higher- v states is small due to the nearly vertical transitions from the $X^2\Sigma_{1/2}(v=0)$ state to the $A^2\Pi_{1/2}(v=0)$ state, with a branching ratio of 3.5% [16]) for decay to higher- v levels.

V. CONCLUSIONS

An electrostatic mirror with nearly spectral reflections is described. A design for a deflector of BaF molecules,

which will separate these molecules from other laser-ablation products is presented.

VI. ACKNOWLEDGEMENTS

We acknowledge support from the Gordon and Betty Moore Foundation, the Alfred P. Sloan Foundation, the

John Templeton Foundation (through the Center for Fundamental Physics at Northwestern University), the Natural Sciences and Engineering Council of Canada, the Canada Foundation for Innovation, the Ontario Research Fund and from York University.

[1] E. Wrede, Über die ablenkung von molekularstrahlen elektrischer dipolmoleküle im inhomogenen elektrischen feld, *Zeitschrift für Physik* **44**, 261 (1927).

[2] S. J. Wark and G. I. Opat, An electrostatic mirror for neutral polar molecules, *Journal of Physics B: Atomic, Molecular and Optical Physics* **25**, 4229 (1992).

[3] S. A. Schulz, H. L. Bethlem, J. van Veldhoven, J. Küpper, H. Conrad, and G. Meijer, Microstructured switchable mirror for polar molecules, *Physical review letters* **93**, 020406 (2004).

[4] A. I. G. Flórez, S. A. Meek, H. Haak, H. Conrad, G. Santambrogio, and G. Meijer, An electrostatic elliptical mirror for neutral polar molecules, *Physical Chemistry Chemical Physics* **13**, 18830 (2011).

[5] L. Jing, Y. Zhenghai, H. Shunyong, W. Bin, L. Qinning, Y. Tao, and Y. Jianping, Cold molecular electrostatic surface mirror, *Journal of East China Normal University (Natural Science Edition)* **2020**, 64.

[6] A. C. Vutha, M. Horbatsch, and E. A. Hessels, Orientation-dependent hyperfine structure of polar molecules in a rare-gas matrix: A scheme for measuring the electron electric dipole moment, *Physical Review A* **98**, 032513 (2018).

[7] R. L. Lambo, G. K. Koyanagi, A. Ragyanszki, M. Horbatsch, R. Fournier, and E. A. Hessels, Calculation of the local environment of a barium monofluoride molecule in an argon matrix: a step towards using matrix-isolated BaF for determining the electron electric dipole moment, *Molecular Physics* **121**, e2198044 (2023).

[8] S. J. Li, H. D. Ramachandran, R. Anderson, and A. C. Vutha, Optical control of BaF molecules trapped in neon ice, *New Journal of Physics* **25**, 082001 (2023).

[9] R. L. Lambo, G. K. Koyanagi, M. Horbatsch, R. Fournier, and E. A. Hessels, Calculation of the local environment of a barium monofluoride molecule in a neon matrix, *Molecular Physics* **121**, e2232051 (2023).

[10] Z. Corriveau, R. L. Lambo, D. Heinrich, J. Perez Garcia, N. T. McCall, H.-M. Yau, T. Chauhan, G. K. Koyanagi, A. Marsman, M. C. George, C. H. Storry, M. Horbatsch, and E. A. Hessels, Matrix isolated barium monofluoride: Assembling a sample of BaF molecules for a measurement of the electron electric dipole moment, *ArXiv preprint* (2024).

[11] A. Touwen, J. W. F. van Hofslot, T. Qualm, R. Borchers, R. Bause, H. L. Bethlem, A. Boeschoten, A. Borschevsky, T. H. Fikkens, S. Hoekstra, K. Jungmann1, V. R. Marshall, T. B. Meijknecht, M. C. Mooij, R. G. E. Timmermans, W. Ubachs, and L. Willmann, Manipulating a beam of barium fluoride molecules using an electrostatic hexapole, *New Journal of Physics* **26**, 073054 (2024).

[12] M. Peter and M. W. P. Strandberg, High-field Stark effect in linear rotors, *Journal of Chemical Physics* **26**, 1657 (1957).

[13] A. Marsman, D. Heinrich, M. Horbatsch, and E. A. Hessels, Large optical forces on a barium monofluoride molecule using laser pulses for absorption and stimulated emission: A full density-matrix simulation, *Physical Review A* **107**, 032811 (2023).

[14] A. Marsman, M. Horbatsch, and E. A. Hessels, Deflection of barium monofluoride molecules using the bichromatic force: A density-matrix simulation, *Physical Review A* **108**, 012811 (2023).

[15] S. Truppe, M. Hambach, S. M. Skoff, N. E. Bulleid, J. S. Bumby, R. J. Hendricks, E. A. Hinds, B. E. Sauer, and M. R. Tarbutt, A buffer gas beam source for short, intense and slow molecular pulses, *J. Modern Optics* **65**, 648 (2018).

[16] Y. Hao, L. F. Paštka, L. Visscher, P. Aggarwal, H. L. Bethlem, A. Boeschoten, A. Borschevsky, M. Denis, K. Esajas, S. Hoekstra, K. Jungmann, V. R. Marshall, T. B. Meijknecht, M. C. Mooij, R. G. E. Timmermans, A. Touwen, W. Ubachs, L. Willmann, Y. Yin, and A. Zappa1, High accuracy theoretical investigations of CaF, SrF, and BaF and implications for laser-cooling, *The Journal of Chemical Physics* **151**, 034302 (2019).